

# Joint Learning of Saliency Detection and Weakly Supervised Semantic Segmentation

Yu Zeng, Yunzhi Zhuge, Huchuan Lu\*, Lihe Zhang  
Dalian University of Technology, China

{zengyu, zgyz}@mail.dlut.edu.cn, {lhchuan, zhanglihe}@dlut.edu.cn,

## Abstract

*Existing weakly supervised semantic segmentation (WSSS) methods usually utilize the results of pre-trained saliency detection (SD) models without explicitly modelling the connections between the two tasks, which is not the most efficient configuration. Here we propose a unified multi-task learning framework to jointly solve WSSS and SD using a single network, i.e. saliency and segmentation network (SS-Net). SSNet consists of a segmentation network (SN) and a saliency aggregation module (SAM). For an input image, SN generates the segmentation result and, SAM predicts the saliency of each category and aggregating the segmentation masks of all categories into a saliency map. The proposed network is trained end-to-end with image-level category labels and class-agnostic pixel-level saliency labels. Experiments on PASCAL VOC 2012 segmentation dataset and four saliency benchmark datasets show the performance of our method compares favorably against state-of-the-art weakly supervised segmentation methods and fully supervised saliency detection methods.*

## 1. Introduction

Semantic image segmentation is an important and challenging task of computer vision, of which the goal is to predict a category label for every image pixel. Recently, convolutional neural networks (CNNs) have achieved remarkable success in semantic image segmentation [33, 8, 7, 31, 2, 6]. Due to the expensive cost for annotating semantic segmentation labels to train CNNs, weakly supervised learning has attracted increasing interest, resulting in various weakly supervised semantic segmentation (WSSS) methods. Saliency detection (SD) aims at identifying the most distinct objects or regions in an image, which has helped many computer vision tasks such as scene classification [41], image retrieval [16], visual tracking [34], to name a few. With the success of deep CNNs, it has been made a lot of at-

tempts to use deep CNNs or deep features for saliency detection [14, 57, 58, 64, 56, 24, 12, 11].

The two tasks both require to generate accurate pixel-wise masks. Hence, they have close connections. On the one hand, given the saliency map of an image, the computation load of a segmentation model can be reduced because of avoiding processing background. On the other hand, given the segmentation result of an image, the saliency map can be readily derived by selecting the salient category. Therefore, many existing WSSS [23, 49, 50, 36, 18, 51, 48, 13] methods have greatly benefited from SD. It is a widespread practice to exploit class activation maps (CAMs) [63] for locating the objects of each category and use SD methods for selecting background regions. For example, Wei *et al.* [51] use CAMs of a classification network with different dilated convolutional rates to find object regions, and use saliency maps of [52] to find background regions for training a segmentation model. Wang *et al.* [48] use saliency maps of [19] to refine object regions produced by classification networks.

However, those WSSS methods simply utilize the results of pre-trained saliency detection models, which is not the most efficient configuration. On the one hand, they use SD methods as a pre-processing step to generate annotations for training their segmentation models while ignoring the interactions between SD and WSSS, which blocks the WSSS models from fully exploiting the segmentation cues of the strong saliency annotations. On the other hand, heuristic rules are usually required for selecting background regions according to the results of SD models, thereby complicating the training process and leading to a not end-to-end manner.

In this paper, we propose a unified, end-to-end training framework to solve both SD and WSSS tasks jointly. Unlike most existing WSSS methods that used pre-trained saliency detection models, we directly take advantage of pixel-level saliency labels. The core motive is to utilize semantic information of the image-level category labels and the segmentation cues of the category-agnostic saliency labels. The image-level category labels can make a CNN recognize the

\*Corresponding author.

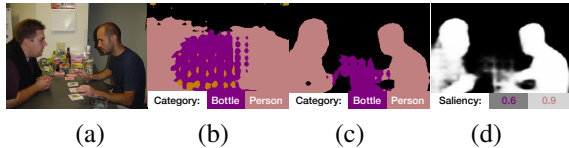


Figure 1. (a) input image. (b) segmentation results predicted by the model trained with only image-level labels. (c) segmentation results predicted by our method. (d) saliency map predicted by our method.

semantic categories, but they do not contain any spatial information, which is essential for segmentation. Although it has been suggested that CNNs trained with image-level labels are also informative of object locations, only a coarse spatial distribution can be inferred, as shown in the first row of Figure 1. We solve this problem with the pixel-level saliency labels. Through explicitly modelling the connection between SD and WSSS, we derive the saliency maps from the segmentation results and minimize the loss between them and the saliency ground-truth. So that the CNN has to precisely cut the recognized objects so as to make the derived saliency maps match the ground-truth.

Specifically, we propose a saliency and segmentation network (SSNet), which includes a segmentation network (SN) and a saliency aggregation module (SAM). For an input image, SN generates the segmentation results, as shown in The second column of Figure 1. SAM predicts the saliency score of each category and then aggregates the segmentation masks of all categories into a saliency map according to their saliency scores, which bridges the gap between semantic segmentation and saliency detection. As shown in the third column of Figure 1, given the segmentation map and saliency score of each category, saliency detection result can be generated by highlighting the masks of salient objects (*e.g.*, the mask of persons in the third column) and suppressing the masks of the objects of low salience (*e.g.*, the mask of bottles in the third column). When training, the loss is computed between the segmentation results and the image-level category labels as well as the saliency maps and the saliency ground-truth.

Our approach has several advantages. First, compared with existing WSSS methods that exploit pre-trained SD models for pre-processing, our method explicitly models the relationships between saliency and segmentation, which can transfer the learned segmentation knowledge from class-agnostic image-specific saliency categories with pixel-level annotations to unseen semantic categories with only image-level annotations. Second, as a low-level vision task, annotating pixel-level ground truth for saliency detection is less expensive than semantic segmentation. Therefore, compared with fully supervised segmentation methods, our method is trained with image-level category labels and saliency annotations, requiring less labeling cost.

Third, compared with existing segmentation or saliency methods, our method can simultaneously predict the segmentation results and saliency results using a single model, with most parameters shared between the two tasks.

In summary, our main contributions are three folds:

- We propose a unified end-to-end framework for both SD and WSSS tasks, in which segmentation is split into two learning tasks respectively based on image-level category labels and pixel-level saliency annotations.
- We design a saliency aggregation module to explicitly bridge the two tasks, through which WSSS can directly benefit from saliency inference and vice versa.
- The experiments on the PASCAL VOC 2012 segmentation benchmark and four saliency benchmarks demonstrate the effectiveness of the proposed method. It achieves favorable performance against weakly supervised semantic segmentation methods and fully supervised saliency detection methods. We make our code and models available for further researches<sup>12</sup>.

## 2. Related work

### 2.1. Saliency detection

Earlier saliency detection methods used low-level features and heuristic priors [55, 20] to detect salient objects, which were not robust to complex scenes. Recently, deep learning based methods have achieved remarkable performance improvements. Incipient deep learning based methods usually used regions as computation units, such as superpixels, image patches, and region proposals. Wang *et al.* [45] trained two neural networks that estimate saliency of image patches and regional proposals respectively. Li and Yu [27] used CNNs to extract multi-scale features and predict the saliency of each superpixel. Inspired by the success of fully convolutional network (FCN) [33] on semantic segmentation, some methods have been proposed to exploit fully convolutional structure for pixel-wise saliency prediction. Liu and Han [32] proposed a deep hierarchical network to learn a coarse global saliency map and then progressively refine it. Wang *et al.* [47] proposed a recurrent FCN incorporates saliency priors. Zhang *et al.* [60] propose to make CNNs learn deep uncertain convolutional features (UCF) to encourage the robustness and accuracy of saliency detection. Zhang *et al.* [61] proposed an attention guided network which selectively integrates multi-level contextual information in a progressive manner. Chen *et al.* [4] proposed reverse attention to guide residual feature learning in a top-down manner for saliency detection. All of the above saliency detection methods trained fully supervised models

<sup>1</sup><https://github.com/zengxianyu/jsws>

<sup>2</sup><http://ice.dlut.edu.cn/lu/>

for a single task. Although our method slightly increases labeling cost, it achieves state-of-the-art performance in both saliency detection and semantic segmentation.

## 2.2. Segmentation with weak supervision

In recent years, a lot of weakly supervised semantic segmentation methods have been proposed to alleviate the cost of labeling. Various supervision has been exploited, such as the image-level labels, bounding boxes, scribbles, *etc.* Among all kinds of weak supervision, the weakest one, *i.e.*, image-level supervision, has attracted the most attention. In image-level weakly supervised segmentation, some methods exploited results of the pre-trained saliency detection models. A simple-to-complex method was presented in [50], in which an initial segmentation model is trained with simple images using saliency maps for supervision. Then the ability of the segmentation model is enhanced by progressively including samples of increasing complexity. Wei *et al.* [49] iteratively used CAM [63] to discover object regions and used saliency detection results of [19] to find background regions to train the segmentation model. Oh *et al.* [36] used an image classifier to find the high confidence points over the objects classes, *i.e.* object seeds, and exploit a CNN-based saliency detection model to find the masks corresponding to some of the detected object seeds. Then these class-specific masks were used to train a segmentation model. Wei *et al.* [51] used a classification network with convolutional blocks of different dilated rates to find object regions and used saliency detection results of [52] to find background regions to train a segmentation model. Wang *et al.* [48] started from the object regions produced by classification networks. The object regions were expanded using the mined features and refined using saliency maps produced by [19]. Then the refined object regions were used as supervision to train a segmentation network. The above weakly supervised segmentation methods all exploited results of pre-trained saliency detection models, either using the existing models or separately training their saliency models and segmentation models. The proposed method has two main differences from these methods. First, these methods used pre-trained saliency detection models, while we directly exploit strong saliency annotations and work in an end-to-end manner. Second, in these methods, saliency detection was used as a pre-processing step to generate training data for segmentation. In contrast, we simultaneously solve saliency detection and semantic segmentation using a single model, of which most parameters are shared between the two tasks.

## 2.3. Multi-task learning

Multi-task learning has been used in a wide range of computer vision problems. Teichman *et al.* [43] proposed an approach to joint classification, detection, and segmenta-

tion using a unified architecture where the encoder is shared among the three tasks. Kokkinos [22] proposed an UberNet that jointly handles low-, mid-, high-level tasks including boundary detection, normal estimation, saliency estimation, semantic segmentation, human part segmentation, semantic boundary detection, region proposal generation, and object detection. Eigen and Fergus [9] used a multiscale CNN to address three different computer vision tasks: depth prediction, surface normal estimation, and semantic labeling. Xu *et al.* [53] proposed a PAD-Net that first solves several auxiliary tasks ranging from low level to high level, and then used the predictions as multi-modal input for the final task. The models above all worked in full supervision setting. In contrast, we jointly learn to solve a task in weak supervision setting and another task in full supervision setting.

## 3. The proposed approach

In this section, we detail the joint learning framework for simultaneous saliency detection and semantic segmentation. We first give an overview of the proposed saliency and segmentation network (SSNet). Then we describe the details of the segmentation network (SN) and the saliency aggregation module (SAM) in Section 3.2 and 3.3. Finally, we present the joint learning strategy in Section 3.4. Figure 2 illustrates the overall architecture of the proposed method.

### 3.1. Network overview

We design two variants of SSNet, *i.e.* SSNet-1, and SSNet-2, for two training stages, respectively. In the first training stage, the SSNet-1 is trained with pixel-level saliency annotations and image-level semantic category labels. In the second stage, the SSNet-2 is trained with saliency annotations and image-level semantic category labels as well as semantic segmentation results predicted by SSNet-1. Both the SSNet-1 and SSNet-2 consist of a segmentation network (SN) and a saliency aggregation module (SAM). Given an input image, SN predicts a segmentation result. SAM predicts a saliency score for each semantic class and aggregates the segmentation map into a single channel saliency map according to the saliency score of each class. Both the SSNet-1 and SSNet-2 are trained end-to-end.

### 3.2. Segmentation networks

The segmentation network consists of a feature extractor to extract features from the input image and several convolution layers to predict segmentation results given the features. Feature extractors of our networks are designed based on state-of-the-art CNN architectures for image recognition, *e.g.*, VGG [42] and DenseNet [17], which typically contain five convolutional blocks for feature extraction and a fully connected classifier. We remove the fully connected

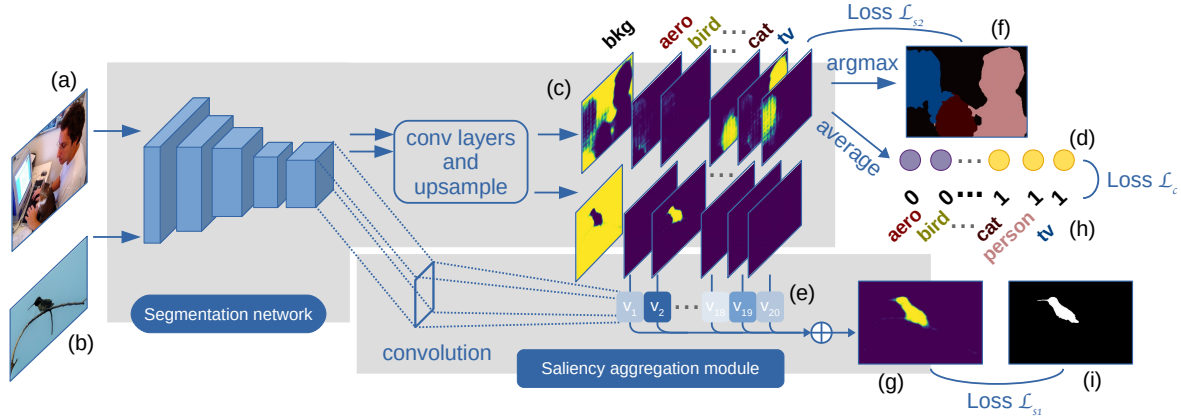


Figure 2. An overview of the proposed method. Our model is trained with (a) *images annotated with category labels* and (b) *images with saliency ground-truth*. For an input image, the segmentation network generates a (c) *segmentation results*, of which the average over spatial locations indicates (d) *the probability of each category*. The saliency aggregation module predicts (e) *saliency score of each category* to aggregate segmentation masks of all categories into a (g) *saliency map*. In the first training stage, the network is trained with the (h) *category labels* and (i) *saliency ground truth*. In the second training stage, the network is trained with (f) *predicted segmentation results* by the model trained in the first stage and the saliency ground truth.

classifier and use the convolutional blocks as our feature extractor. To obtain larger feature maps, we remove the down-sampling operator from the last two convolution blocks and use dilated convolution to retain the original receptive field. The feature extractor generates feature maps of 1/8 the input image size. We resize the input images to  $256 \times 256$ , so the resulted feature maps are  $32 \times 32$  in spatial scale.

In the first training stage, the only available semantic supervision cue is the image-level labels. Trained with image-level labels, a coarse spatial distribution of each class can be inferred but it is difficult to train a sophisticated model. Therefore, we use a relatively simple structure in SSNet-1 for generating segmentation results, *i.e.* a  $1 \times 1$  convolution layer. The predicted  $C$ -channel segmentation map and one-channel background map are of 1/8 the input image size, in which  $C$  is the number of semantic classes. Each element of the segmentation map and background map is a value in  $[0, 1]$ . The values of all classes sum to 1 for each pixel. Then the segmentation results are upsampled by a deconvolution layer to the input image size. In the second training stage, the segmentation results of SSNet-1 can be used for training, which is a stronger supervision cue. Therefore, we can use a more complex segmentation network to generate finer segmentation results. Inspired by Deeplab [3], we use four  $3 \times 3$  convolution layers with dilation rate 6, 12, 18, 24 in SSNet-2 and take the summation of their outputs as the segmentation results. Similar to SSNet-1, these segmentation results are of 1/8 the input image size, and are upsampled by a deconvolution layer to the input size.

### 3.3. Saliency aggregation

We design a saliency aggregation module (SAM) as a bridge between the two tasks so that the segmentation network can make use of the class-agnostic pixel-level saliency labels and generate more accurate segmentation results. This module takes the  $32 \times 32$  outputs  $F$  of the feature extractor, and generates a  $C$ -dimensional vector  $v$  with a  $32 \times 32$  convolution layer and a sigmoid function, of which each element  $v_i$  is the saliency score of the  $i$ -th category. Then the saliency map  $S$  is given by a weighted sum of the segmentation masks of all classes:

$$S = \sum_{i=1}^C v_i \cdot H_i, \quad (1)$$

where  $H_i$  denotes the  $i$ -th channel of the segmentation results encoding the spatial distribution of the  $i$ -th category, which are the output of the segmentation network.

### 3.4. Jointly learning of saliency and segmentation

We use two training sets to train the proposed SSNet: the saliency dataset with pixel-level saliency annotations, and the classification dataset with image-level semantic category labels. Let  $\mathcal{D}_s = \{(X^n, Y^n)\}_{n=1}^{N_s}$  denote the saliency dataset, in which  $X^n$  is the image, and  $Y^n$  is the ground truth. Each element of  $Y^n$  is either 1 or 0, representing the corresponding pixel belongs to salient objects or background, respectively. The classification dataset is denoted as  $\mathcal{D}_c = \{(X^n, t^n)\}_{n=1}^{N_c}$ , in which  $X^n$  is the image, and  $t^n$  is the one-hot encoding of the categories of the image.

For an input image, the segmentation network generates its segmentation result, from which the probability of each



category can be derived by averaging the segmentation results over spatial locations. We compute the loss between these values and the ground-truth category labels and backward propagate it to make the segmentation results semantically correct, *i.e.*, the semantic categories appearing in the input image are correctly recognized. This loss, denoted as  $\mathcal{L}_c$ , is defined as follow,

$$\mathcal{L}_c = -\frac{1}{N_c} \sum_{n=1}^{N_c} \left[ \sum_{i=1}^C t_i^n \log \hat{t}_i^n + (1 - t_i^n) \log(1 - \hat{t}_i^n) \right], \quad (2)$$

in which  $t_i^n$  is the  $i$ -th element of  $t^n$ .  $t_i^n = 1$  represents the image  $X^n$  contains objects of the  $i$ -th category, and  $t_i^n = 0$  otherwise.  $\hat{t}_i^n$  is the average over spatial positions of the segmentation maps  $H^n$  of image  $X^n$ , of which each element  $\hat{t}_i^n \in [0, 1]$  represents the predicted probability of the  $i$ -th class objects presenting in the image.

The image-level category labels can make the segmentation network recognize the semantic categories, but they do not contain any spatial information, which is essential for segmentation. We solve this problem with the pixel-level saliency labels. As stated in Section 3.3, the SAM generates the saliency score of each category and aggregates the segmentation result into a saliency map. We minimize a loss  $\mathcal{L}_{s1}$  between the derived saliency maps and the ground-truth so that the segmentation network has to precisely cut the recognized objects to make the derived saliency maps match the ground-truth. The loss  $\mathcal{L}_{s1}$  between the saliency maps and the saliency ground-truth is defined as follow,

$$\mathcal{L}_{s1} = -\frac{1}{N_s} \sum_{n=1}^{N_s} \left[ \sum_m y_m^n \log s_m^n + (1 - y_m^n) \log(1 - s_m^n) \right], \quad (3)$$

where  $y_m^n \in \{0, 1\}$  is the value of the  $m$ -th pixel of the saliency ground truth  $Y^n$ .  $s_m^n \in [0, 1]$  is the value of the  $m$ -th pixel in the saliency map of the image  $X^n$ , encoding the predicted probability of the  $m$ -th pixel being salient.

In the first training stage, we train SSNet-1 with the loss  $\mathcal{L}_c + \mathcal{L}_{s1}$ . After having trained SSNet-1, we run it on the classification dataset  $\mathcal{D}_c$  and obtain the  $C + 1$ -channel segmentation results, of which the first  $C$  channels correspond to the  $C$  semantic categories and the last channel corresponds to the background. Then the first  $C$  channels of the segmentation result are cross-channel multiplied with the one-hot class label  $t^n$  to suppress wrong predictions and refined with CRF [25] to enhance spatial smoothness. Finally, we obtain some pseudo labels by assigning each pixel  $m$  of each training image  $X^n \in \mathcal{D}_c$  a class label including the background label corresponding to the maximum value in the refined segmentation result. We define a loss  $\mathcal{L}_{s2}$  between the segmentation results and the pseudo labels as

follow,

$$\mathcal{L}_{s2} = -\frac{1}{N_c} \sum_{n=1}^{N_c} \left[ \sum_{i=1}^{C+1} \sum_{m \in \mathcal{C}_i} \log h_{im}^n \right], \quad (4)$$

in which  $h_{im}^n \in [0, 1]$ ,  $i = 1, \dots, C$  is the value of  $H^n$  at pixel  $m$  and channel  $i$ , representing the probability of pixel  $m$  belonging to the  $i$ -th class. SSNet-2 is trained with the loss  $\mathcal{L}_{s1} + \mathcal{L}_{s2}$ .

## 4. Experiments

### 4.1. Dataset and settings

**Segmentation** For semantic segmentation task, we evaluate the proposed method on the PASCAL VOC 2012 segmentation benchmark [10]. This dataset has 20 object categories and one background category. It is split into a training set of 1,464 images, a validation set of 1,449 images and a test set of 1,456 images. Following the common practice [1, 15, 49], we increase the number of training images to 10,582 by augmentation. We only use image-level labels for training. The performance of our method and other state-of-the-art methods are evaluated on the validation set and test set. The performance for semantic segmentation is evaluated in terms of inter-section-over-union averaged over 21 classes (mIOU) according to the PASCAL VOC evaluation criterion. We obtain the mIOU on the test set by submitting our results to the PASCAL VOC evaluation server.

**Saliency** For saliency detection task, we use the DUT-S training set [46] for training, which has 10,553 images with pixel-level saliency annotations. The proposed method and other state-of-the-art methods are evaluated on four benchmark datasets: ECSSD [54], PASCAL-S [30], HKU-IS [27], SOD [35]. ECSSD contains 1000 natural images with multiple objects of different sizes. PASCAL-S stems from the validation set of PASCAL VOC 2010 segmentation dataset and contains 850 natural images. HKU-IS has 4447 images chosen to include multiple disconnected objects or objects touching the image boundary. SOD has 300 challenging images, of which many images contain multiple objects either with low contrast or touching the image boundary. The performance for saliency detection is evaluated in terms of maximum F-measure and mean absolute error (MAE).

**Training/Testing Settings** We adopt DenseNet-169 [17] pre-trained on ImageNet [5] as the feature extractor of our segmentation network due to its ability to achieve comparable performance with a smaller number of parameters than other architectures. Our network is implemented based on Pytorch framework and trained on two NVIDIA GeForce GTX 1080 Ti GPU. We use Adam optimizer [21] to train our network. We randomly crop a patch of 9/10 of the original image size and rescaled to  $256 \times 256$  when training.

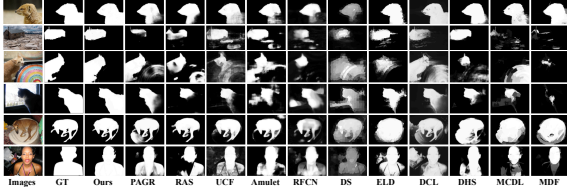


Figure 3. Visual comparison of the proposed method with state-of-the-art fully supervised saliency detection methods.

The batch size is set to 16. We train both the SSNet-1 and SSNet-2 for 10,000 iterations with initial learning rate  $1e-4$ , and decrease the learning rate by 0.5 every 1000 iterations. When testing, the input image is resized to  $256 \times 256$ . Then, the predicted segmentation results and saliency maps are resized to the input size by nearest interpolation. We do not use any post-processing on the segmentation results. We apply CRF [25] to refine the saliency maps.

#### 4.2. Comparison with saliency methods

We compare our method with the following state-of-the-art deep learning based fully supervised saliency detection methods: PAGR (CVPR’18) [61], RAS (ECCV’18) [4], UCF (ICCV’17) [60], Amulet (ICCV’17) [59], RFCN (ECCV’16) [47], DS (TIP’16) [29], ELD (CVPR’16) [26], DCL (CVPR’16) [28], DHS (CVPR’16) [32], MCDL (CVPR’15) [62], MDF (CVPR’15) [27]. Figure 3 shows a visual comparison of our method against state-of-the-art fully supervised saliency detection methods. The comparison in terms of MAE and maximum F-measure is shown in Table 1 and Table 2 respectively. As shown in Table 1, the proposed method achieves the smallest MAE among across all datasets. Maximum F-measure in Table 2 also shows that our method achieves the second largest F-measure in one dataset, and achieves the third largest F-measure in the other three datasets. Together the two metrics, it can be seen that our method achieves state-of-the-art performance in saliency detection task.

#### 4.3. Comparison with segmentation methods

In this section, we compare our method with previous state-of-the-art weakly supervised semantic segmentation methods, *i.e.* MIL (CVPR’15) [38], WSSL [37], RAWK [44], BFBP (ECCV’16) [40], SEC (ECCV’16) [23], AE (CVPR’17) [49], STC (PAMI’17) [50], CBTS (CVPR’17) [39], ESOS (CVPR’17) [36], MCOF (CVPR’18) [48], MDC (CVPR’18) [51]. WSSL uses bounding boxes as supervision, RAWK uses scribbles as supervision, and other methods use image-level categories as supervision. Among the methods using image-level supervision, ESOS exploits the saliency detection results of a deep CNN trained with bounding box annotations. AE, STC, MCOF, MDC use the results of fully supervised

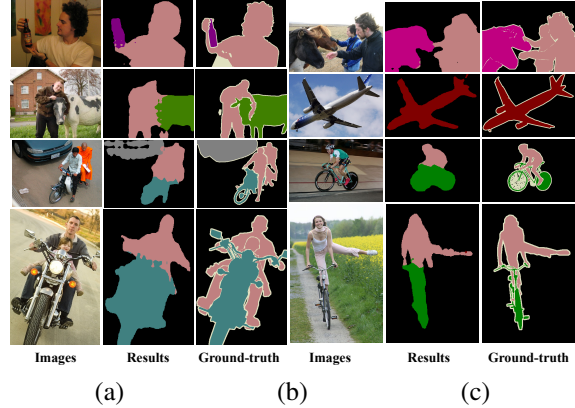


Figure 4. Qualitative results of the proposed method on PASCAL VOC 2012 validation set.

saliency detection models and thus implicitly use pixel level saliency annotations. As some previous methods used VGG16 as its backbone network, we also report the performance of our method using VGG16. It can be seen from Table 3 and Table 4 that our method compares favourably against all the above methods, including methods using stronger supervision such as bounding boxes (WSSL) and scribbles (RAWK). Our method also outperforms the methods *i.e.*, ESOS, AE, STC, MCOF, MDC, that implicitly use saliency annotations by using pre-trained saliency detection models. Compared with these methods, our method simultaneously solves semantic segmentation and saliency detection and can be trained in an end-to-end manner, which is more efficient and easier to train.

#### 4.4. Ablation study

In this section, we analyze the effect of the proposed jointly learning framework. To validate the impact of multitasking, we show the performance of the networks trained in different single-task and multi-task settings.

**Semantic segmentation** The quantitative and the qualitative comparison of the models trained in the different settings for segmentation task is shown in Table 5 and Figure 5 respectively. For the first training stage, we firstly train SSNet-1 in the single-task setting, where only the image-level category labels and  $\mathcal{L}_c$  are used. The resulted model is denoted as SSNet-S, of which the mIOU is shown in the first column of Table 5. Then we add the saliency task to train SSNet-1 in the multi-task setting. In this setting  $\mathcal{L}_c + \mathcal{L}_{s1}$  is used as loss function, with both the image-level category labels and the saliency dataset are used as training data. The resulted model is denoted as SSNet-M, of which mIOU is shown in the second column of Table 5. It can be seen that SSNet-M has a much larger mIOU than SSNet-S, demonstrating that jointly learning saliency detection is of great benefit to WSSS. In the second training

Table 1. Comparison of fully supervised saliency detection methods in terms of MAE (the smaller the better). The best three results are in red, green and blue, respectively.

Methods/Datasets	RAS <sup>18</sup>	PAGR <sup>18</sup>	UCF <sup>17</sup>	Amule <sup>17</sup>	RFCN <sup>16</sup>	DS <sup>16</sup>	ELD <sup>16</sup>	DCL <sup>16</sup>	DHS <sup>16</sup>	MCDL <sup>15</sup>	MDF <sup>15</sup>	Ours
ECSSD	0.056	0.061	0.078	0.059	0.107	0.122	0.079	0.088	0.059	0.101	0.105	0.045
PASCAL-S	0.104	0.093	0.126	0.098	0.118	0.176	0.123	0.125	0.094	0.145	0.146	0.067
HKU-IS	0.045	0.048	0.074	0.052	0.079	0.080	0.074	0.072	0.053	0.092	0.129	0.040
DUTS-test	0.060	0.056	0.117	0.085	0.091	0.090	0.093	0.088	0.067	0.106	0.094	0.052

Table 2. Comparison of fully supervised saliency detection methods in terms of maximum F-measure (the larger the better). The best three results are in red, green and blue, respectively.

Methods/Datasets	RAS <sup>18</sup>	PAGR <sup>18</sup>	UCF <sup>17</sup>	Amule <sup>17</sup>	RFCN <sup>16</sup>	DS <sup>16</sup>	ELD <sup>16</sup>	DCL <sup>16</sup>	DHS <sup>16</sup>	MCDL <sup>15</sup>	MDF <sup>15</sup>	Ours
ECSSD	0.921	0.927	0.911	0.915	0.890	0.882	0.867	0.890	0.907	0.837	0.832	0.919
PASCAL-S	0.837	0.856	0.828	0.837	0.837	0.765	0.773	0.805	0.829	0.743	0.768	0.851
HKU-IS	0.913	0.918	0.886	0.895	0.892	0.865	0.839	0.885	0.890	0.808	0.861	0.907
DUTS-test	0.831	0.855	0.771	0.778	0.784	0.777	0.738	0.782	0.807	0.672	0.730	0.832

Table 3. Comparison of WSSS methods on PASCAL VOC 2012 validation set. \* marks the methods implicitly use saliency annotations by using pre-trained saliency detection models. † and ‡ mark the methods use box supervisions and scribble supervisions, respectively. Ours: our method with Densenet169-based feature extractor. Ours-VGG: our method with VGG16-based feature extractor. MCOF-Res: MCOF with ResNet101-based feature extractor. MCOF-VGG: MCOF with VGG16-based feature extractor. The best three results are in red, green and blue.

Method	bkg	areo	bike	bird	boat	bottle	bus	car	cat	chair	cow	table	dog	horse	mbk	person	plant	sheep	sofa	train	tv	mean	
MIL <sup>15</sup>	74.7	38.8	19.8	27.5	21.7	32.8	40.0	50.1	47.1	7.2	44.8	15.8	49.4	47.3	36.6	36.4	24.3	44.5	21.0	31.5	41.3	35.8	
WSSL <sup>†15</sup>	-	-	-	-	-	-	-	-	-	-	-	-	-	-	-	-	-	-	-	-	-	-	60.6
BFBP <sup>16</sup>	79.2	60.1	20.4	50.7	41.2	46.3	62.6	49.2	62.3	13.3	49.7	38.1	58.4	49.0	57.0	48.2	27.8	55.1	29.6	54.6	26.6	46.6	
SEC <sup>16</sup>	82.2	61.7	26.0	60.4	25.6	45.6	70.9	63.2	72.2	20.9	52.9	30.6	62.8	56.8	63.5	57.1	32.2	60.6	32.3	44.8	42.3	50.7	
RAWK <sup>‡17</sup>	-	-	-	-	-	-	-	-	-	-	-	-	-	-	-	-	-	-	-	-	-	-	61.4
STC <sup>*17</sup>	84.5	68.0	19.5	60.5	42.5	44.8	68.4	64.0	64.8	14.5	52.0	22.8	58.0	55.3	57.8	60.5	40.6	56.7	23.0	57.1	31.2	49.8	
AE <sup>*17</sup>	-	-	-	-	-	-	-	-	-	-	-	-	-	-	-	-	-	-	-	-	-	-	55.0
CBTS <sup>17</sup>	85.8	65.2	29.4	63.8	31.2	37.2	69.6	64.3	76.2	21.4	56.3	29.8	68.2	60.6	66.2	55.8	30.8	66.1	34.9	48.8	47.1	52.8	
ESOS <sup>*17</sup>	-	-	-	-	-	-	-	-	-	-	-	-	-	-	-	-	-	-	-	-	-	-	55.7
MCOF-Res <sup>*18</sup>	87.0	78.4	29.4	68.0	44.0	67.3	80.3	74.1	82.2	21.1	70.7	28.2	73.2	71.5	67.2	53.0	47.7	74.5	32.4	71.0	45.8	60.3	
MCOF-VGG <sup>*18</sup>	85.8	74.1	23.6	66.4	36.6	62.0	75.5	68.5	78.2	18.8	64.6	29.6	72.5	61.6	63.1	55.5	37.7	65.8	32.4	68.4	39.9	56.2	
MDC <sup>*18</sup>	89.5	85.6	34.6	75.8	61.9	65.8	67.1	73.3	80.2	15.1	69.9	8.1	75.0	68.4	70.9	71.5	32.6	74.9	24.8	73.2	50.8	60.4	
Ours-VGG	89.1	71.5	31.0	74.2	58.6	63.6	78.1	69.2	74.4	10.7	63.6	9.8	66.4	64.4	66.6	64.8	27.5	69.2	24.3	71.0	50.9	57.1 <sup>a</sup>	
Ours	90.0	77.4	37.5	80.7	61.6	67.9	81.8	69.0	83.7	13.6	79.4	23.3	78.0	75.3	71.4	68.1	35.2	78.2	32.5	75.5	48.0	63.3 <sup>b</sup>	

<sup>a</sup><http://host.robots.ox.ac.uk:8080/anonymous/F5E3DJ.html>

<sup>b</sup><http://host.robots.ox.ac.uk:8080/anonymous/AOZU76.html>

stage, the training data for SSNet-2 consists of two splits: the one is the predictions of SSNet-1, and the other is the saliency dataset. In order to verify the contribution of each split, we train SSNet-2 in three settings: 1) train with only the predictions of SSNet-S using the  $\mathcal{L}_{s_2}$  as loss function, 2) train with only the predictions of SSNet-M using the  $\mathcal{L}_{s_2}$  as loss function, and 3) train with the predictions of SSNet-M and the saliency dataset using  $\mathcal{L}_{s_1} + \mathcal{L}_{s_2}$  as loss function. The resulted models under the three settings is denoted as SSNet-SS, SSNet-MS and SSNet-MM, of which the mIOU scores are shown in the third to the fifth column of Table 5. From the comparison of SSNet-SS and SSNet-MS, it can be seen that the model trained with the multi-task setting in the first training stage can provide better training data for the second training stage. The com-

parison of SSNet-MS and SSNet-MM shows that when trained with the same pixel-level segmentation labels, the model trained in the multi-task setting is still better than the single-task setting.

**Saliency detection** To study the effect of jointly learning for saliency detection, we compare the performance of SSNet-2 trained in multi-task settings and single-task settings. We firstly train SSNet-2 only for saliency detection task, resulting in a model denoted as SSNet-2S, of which the maximum F-measure and MAE are shown in the first column of Table 6. Then we run the model SSNet-MM mentioned above on saliency dataset, and the resulted F-measure and MAE are shown in the second column of Table 6. As can be seen, the models trained in multi-task setting has a comparable performance to the model trained in single-task setting,

Table 4. Comparison of WSSS methods on PASCAL VOC 2012 test set. \* marks the methods implicitly use saliency annotations by using pre-trained saliency detection models. † and ‡ mark the methods use box supervisions and scribble supervisions, respectively. Ours: our method with Densenet169-based feature extractor. Ours-VGG: our method with VGG16-based feature extractor. MCOF-Res: MCOF with ResNet101-based feature extractor. MCOF-VGG: MCOF with VGG16-based feature extractor. The best three are in red, green, blue.

Method	bkg	areo	bike	bird	boat	bottle	bus	car	cat	chair	cow	table	dog	horse	mbk	person	plant	sheep	sofa	train	tv	mean
MIL <sup>15</sup>	74.7	38.8	19.8	27.5	21.7	32.8	40.0	50.1	47.1	7.2	44.8	15.8	49.4	47.3	36.6	36.4	24.3	44.5	21.0	31.5	41.3	35.8
WSSL <sup>†</sup> <sub>15</sub>	-	-	-	-	-	-	-	-	-	-	-	-	-	-	-	-	-	-	-	-	-	62.2
BFBP <sup>16</sup>	80.3	57.5	24.1	66.9	31.7	43.0	67.5	48.6	56.7	12.6	50.9	42.6	59.4	52.9	65.0	44.8	41.3	51.1	33.7	44.4	33.2	48.0
SEC <sup>16</sup>	83.5	56.4	28.5	64.1	23.6	46.5	70.6	58.5	71.3	23.2	54.0	28.0	68.1	62.1	70.0	55.0	38.4	58.0	39.9	38.4	48.3	51.7
STC <sup>*16</sup>	85.2	62.7	21.1	58.0	31.4	55.0	68.8	63.9	63.7	14.2	57.6	28.3	63.0	59.8	67.6	61.7	42.9	61.0	23.2	52.4	33.1	51.2
AE <sup>*17</sup>	-	-	-	-	-	-	-	-	-	-	-	-	-	-	-	-	-	-	-	-	-	55.7
CBTS <sup>17</sup>	85.7	58.8	30.5	67.6	24.7	44.7	74.8	61.8	73.7	22.9	57.4	27.5	71.3	64.8	72.4	57.3	37.0	60.4	42.8	42.2	50.6	53.7
ESOS <sup>*17</sup>	-	-	-	-	-	-	-	-	-	-	-	-	-	-	-	-	-	-	-	-	-	56.7
MCOF-Res <sup>*18</sup>	88.2	80.8	31.4	70.9	34.9	65.7	83.5	75.1	79.0	22.0	70.3	31.7	77.7	72.9	77.1	56.9	41.8	74.9	36.6	71.2	42.6	61.2
MCOF-VGG <sup>*18</sup>	86.8	73.4	26.6	60.6	31.8	56.3	76.0	68.9	79.4	18.8	62.0	36.9	74.5	66.9	74.9	58.1	44.6	68.3	36.2	64.2	44.0	57.6
MDC <sup>*18</sup>	89.8	78.4	36.2	82.1	52.4	61.7	64.2	73.5	78.4	14.7	70.3	11.9	75.3	74.2	81.0	72.6	38.8	76.7	24.6	70.7	50.3	60.8
Ours-VGG	89.2	75.4	31.0	72.3	45.0	56.6	79.3	73.2	73.9	14.1	64.4	19.7	69.5	71.1	76.7	64.7	41.8	70.9	27.5	68.2	46.6	58.6 <sup>a</sup>
Ours	90.4	85.4	37.9	77.2	48.2	64.5	83.9	74.8	83.4	15.9	72.4	34.3	80.0	77.3	78.5	69.0	41.9	76.3	38.3	72.3	48.2	64.3 <sup>b</sup>

<sup>a</sup><http://host.robots.ox.ac.uk:8080/anonymous/YTXEXK.html>

<sup>b</sup><http://host.robots.ox.ac.uk:8080/anonymous/PHYZSJ.html>

where the former has a larger maximum F-measure and the later is better in terms of MAE. Therefore, it is safe to conclude that conduct jointly learning of semantic segmentation dose not harm the performance on saliency detection. This result validates the superiority of the proposed jointly learning framework considering its great benefit to semantic segmentation.

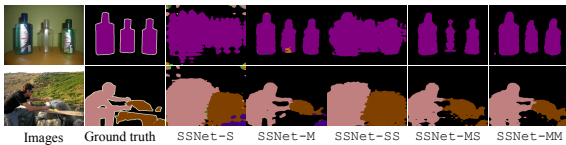


Figure 5. Visual effect of the segmentation results of the models trained in different settings. Images: input images. Ground truth: segmentation ground truth. SSNet-S: results of SSNet-1 trained in single-task setting. SSNet-M: results of SSNet-1 trained in multi-task setting. SSNet-SS: results of SSNet-2 trained in single task setting using the predictions of SSNet-S. SSNet-MS: results of SSNet-2 trained in single-task setting using the predictions of SSNet-M. SSNet-MM: results of SSNet-2 trained in multi-task setting using the predictions of SSNet-M.

Table 5. Comparison of the models trained in different settings on semantic segmentation task. S and M represent single-task training and multi-task training respectively. Larger mIOU indicates better performance. The best results are in bold.

training stage	training strategy				
stage 1	S	M	S	M	M
stage 2			S	S	M
mIOU	33.1	57.1	47.1	62.7	<b>63.3</b>

Table 6. Comparison of the models trained in different settings on saliency detection task (evaluated on ECSSD dataset). S and M represent single-task training and multi-task training respectively. CRF represents the results after CRF post processing. Larger max  $F_\beta$  and smaller MAE indicate better performance. The best results are in bold.

	training strategy		
	S	M	M
MAE	0.046	0.047	<b>0.045</b> (CRF)
max $F_\beta$	0.899	0.912	<b>0.919</b> (CRF)

## 5. Conclusion

This paper presents a joint learning framework for saliency detection (SD) and weakly supervised semantic segmentation (WSSS) using a single model, *i.e.* the saliency and segmentation network (SSNet). Compared with WSSS methods exploiting pre-trained SD models, our method makes full use of segmentation cues from saliency annotations and is easier to train. Compared with existing fully supervised SD methods, our method can provide more informative results. Experiments shows that our method achieves state-of-the-art performance among both fully supervised SD methods and WSSS methods.

## Acknowledgements

Supported by the National Natural Science Foundation of China #61725202, #61829102, #61751212, #61876202, Fundamental Research Funds for the Central Universities under Grant #DUT19GJ201 and Dalian Science and Technology Innovation Foundation #2019J12GX039.



## References

- [1] Liang-Chieh Chen, George Papandreou, Iasonas Kokkinos, Kevin Murphy, and Alan L Yuille. Semantic image segmentation with deep convolutional nets and fully connected crfs. *arXiv preprint arXiv:1412.7062*, 2014. 5
- [2] Liang-Chieh Chen, George Papandreou, Iasonas Kokkinos, Kevin Murphy, and Alan L Yuille. Deeplab: Semantic image segmentation with deep convolutional nets, atrous convolution, and fully connected crfs. *IEEE transactions on pattern analysis and machine intelligence*, 40(4):834–848, 2017. 1
- [3] Liang-Chieh Chen, George Papandreou, Iasonas Kokkinos, Kevin Murphy, and Alan L Yuille. Deeplab: Semantic image segmentation with deep convolutional nets, atrous convolution, and fully connected crfs. *IEEE transactions on pattern analysis and machine intelligence*, 40(4):834–848, 2018. 4
- [4] Shuhan Chen, Xiuli Tan, Ben Wang, and Xuelong Hu. Reverse attention for salient object detection. In *European conference on computer vision*, 2018. 2, 6
- [5] Jia Deng, Wei Dong, Richard Socher, Li-Jia Li, Kai Li, and Li Fei-Fei. Imagenet: A large-scale hierarchical image database. In *IEEE conference on computer vision and pattern recognition*, 2009. 5
- [6] Henghui Ding, Xudong Jiang, Ai Qun Liu, Nadia Magnenat Thalmann, and Gang Wang. Boundary-aware feature propagation for scene segmentation. In *Proceedings of the International Conference on Computer Vision*, 2019. 1
- [7] Henghui Ding, Xudong Jiang, Bing Shuai, Ai Qun Liu, and Gang Wang. Context contrasted feature and gated multi-scale aggregation for scene segmentation. In *Proceedings of the IEEE Conference on Computer Vision and Pattern Recognition*, pages 2393–2402, 2018. 1
- [8] Henghui Ding, Xudong Jiang, Bing Shuai, Ai Qun Liu, and Gang Wang. Semantic correlation promoted shape-variant context for segmentation. In *IEEE conference on computer vision and pattern recognition*, 2019. 1
- [9] David Eigen and Rob Fergus. Predicting depth, surface normals and semantic labels with a common multi-scale convolutional architecture. In *IEEE international conference on computer vision*, 2015. 3
- [10] Mark Everingham, SM Ali Eslami, Luc Van Gool, Christopher KI Williams, John Winn, and Andrew Zisserman. The pascal visual object classes challenge: A retrospective. *International journal of computer vision*, 111(1):98–136, 2015. 5
- [11] Deng-Ping Fan, Ming-Ming Cheng, Jiang-Jiang Liu, Shang-Hua Gao, Qibin Hou, and Ali Borji. Salient objects in clutter: Bringing salient object detection to the foreground. pages 186–202. Springer, 2018. 1
- [12] Deng-Ping Fan, Wenguan Wang, Ming-Ming Cheng, and Jianbing Shen. Shifting more attention to video salient object detection. In *CVPR*, pages 8554–8564, 2019. 1
- [13] Ruochen Fan, Qibin Hou, Ming-Ming Cheng, Gang Yu, Ralph R Martin, and Shi-Min Hu. Associating inter-image salient instances for weakly supervised semantic segmentation. In *European conference on computer vision*, 2018. 1
- [14] Mengyang Feng, Huchuan Lu, and Errui Ding. Attentive feedback network for boundary-aware salient object detection. In *IEEE Conference on Computer Vision and Pattern Recognition*, 2019. 1
- [15] Bharath Hariharan, Pablo Arbeláez, Lubomir Bourdev, Subhransu Maji, and Jitendra Malik. Semantic contours from inverse detectors. In *International Conference on Computer Vision*, 2011. 5
- [16] Junfeng He, Jinyuan Feng, Xianglong Liu, Tao Cheng, Tai-Hsu Lin, Hyunjin Chung, and Shih-Fu Chang. Mobile product search with bag of hash bits and boundary reranking. In *IEEE conference on computer vision and pattern recognition*, 2012. 1
- [17] Gao Huang, Zhuang Liu, Laurens Van Der Maaten, and Kilian Q Weinberger. Densely connected convolutional networks. In *IEEE conference on computer vision and pattern recognition*, 2017. 3, 5
- [18] Zilong Huang, Xinggang Wang, Jiasi Wang, Wenyu Liu, and Jingdong Wang. Weakly-supervised semantic segmentation network with deep seeded region growing. In *IEEE conference on computer vision and pattern recognition*, 2018. 1
- [19] Huaizu Jiang, Jingdong Wang, Zejian Yuan, Yang Wu, Nanning Zheng, and Shipeng Li. Salient object detection: A discriminative regional feature integration approach. In *IEEE conference on computer vision and pattern recognition*, 2013. 1, 3
- [20] Zhuolin Jiang and Larry S Davis. Submodular salient region detection. In *IEEE conference on computer vision and pattern recognition*, 2013. 2
- [21] Diederik Kingma and Jimmy Ba. Adam: A method for stochastic optimization. *arXiv preprint arXiv:1412.6980*, 2014. 5
- [22] Iasonas Kokkinos. Ubernet: Training a universal convolutional neural network for low-, mid-, and high-level vision using diverse datasets and limited memory. In *IEEE conference on computer vision and pattern recognition*, 2017. 3
- [23] Alexander Kolesnikov and Christoph H Lampert. Seed, expand and constrain: Three principles for weakly-supervised image segmentation. In *European conference on computer vision*, 2016. 1, 6
- [24] Yuqiu Kong, Jianming Zhang, Huchuan Lu, and Xiuping Liu. Exemplar-aided salient object detection via joint latent space embedding. *IEEE Transactions on Image Processing*, 27(10):5167–5177, 2018. 1
- [25] Philipp Krähenbühl and Vladlen Koltun. Efficient inference in fully connected crfs with gaussian edge potentials. In *Advances in neural information processing systems*, 2011. 5, 6
- [26] Gayoung Lee, Yu-Wing Tai, and Junmo Kim. Deep saliency with encoded low level distance map and high level features. In *IEEE conference on computer vision and pattern recognition*, 2016. 6
- [27] Guanbin Li and Yizhou Yu. Visual saliency based on multi-scale deep features. In *IEEE conference on computer vision and pattern recognition*, 2015. 2, 5, 6
- [28] Guanbin Li and Yizhou Yu. Deep contrast learning for salient object detection. In *IEEE conference on computer vision and pattern recognition*, 2016. 6

- [29] Xi Li, Liming Zhao, Lina Wei, Ming-Hsuan Yang, Fei Wu, Yueting Zhuang, Haibin Ling, and Jingdong Wang. Deep-saliency: Multi-task deep neural network model for salient object detection. *IEEE transactions on image processing*, 25(8):3919–3930, 2016. 6
- [30] Yin Li, Xiaodi Hou, Christof Koch, James M Rehg, and Alan L Yuille. The secrets of salient object segmentation. In *IEEE conference on computer vision and pattern recognition*, 2014. 5
- [31] Guosheng Lin, Anton Milan, Chunhua Shen, and Ian Reid. Refinenet: Multi-path refinement networks for high-resolution semantic segmentation. In *IEEE conference on computer vision and pattern recognition*, 2017. 1
- [32] Nian Liu and Junwei Han. Dhsnet: Deep hierarchical saliency network for salient object detection. In *IEEE conference on computer vision and pattern recognition*, 2016. 2, 6
- [33] Jonathan Long, Evan Shelhamer, and Trevor Darrell. Fully convolutional networks for semantic segmentation. In *IEEE conference on computer vision and pattern recognition*, 2015. 1, 2
- [34] Vijay Mahadevan, Nuno Vasconcelos, et al. Biologically inspired object tracking using center-surround saliency mechanisms. *IEEE transactions on pattern analysis and machine intelligence*, 35(3):541–554, 2013. 1
- [35] David Martin, Charless Fowlkes, Doron Tal, and Jitendra Malik. A database of human segmented natural images and its application to evaluating segmentation algorithms and measuring ecological statistics. In *IEEE international conference on computer vision*, 2001. 5
- [36] Seong Joon Oh, Rodrigo Benenson, Anna Khoreva, Zeynep Akata, Mario Fritz, and Bernt Schiele. Exploiting saliency for object segmentation from image level labels. In *IEEE conference on computer vision and pattern recognition*, 2017. 1, 3, 6
- [37] George Papandreou, Liang-Chieh Chen, Kevin Murphy, and Alan L Yuille. Weakly-and semi-supervised learning of a dcnn for semantic image segmentation. In *IEEE international conference on computer vision*, 2015. 6
- [38] Pedro O Pinheiro and Ronan Collobert. From image-level to pixel-level labeling with convolutional networks. In *IEEE conference on computer vision and pattern recognition*, 2015. 6
- [39] Anirban Roy and Sinisa Todorovic. Combining bottom-up, top-down, and smoothness cues for weakly supervised image segmentation. In *IEEE conference on computer vision and pattern recognition*, 2017. 6
- [40] Fatemehsadat Saleh, Mohammad Sadegh Aliakbarian, Mathieu Salzmann, Lars Petersson, Stephen Gould, and Jose M Alvarez. Built-in foreground/background prior for weakly-supervised semantic segmentation. In *European conference on computer vision*, 2016. 6
- [41] Christian Siagian and Laurent Itti. Rapid biologically-inspired scene classification using features shared with visual attention. *IEEE transactions on pattern analysis and machine intelligence*, 29(2):300–312, 2007. 1
- [42] Karen Simonyan and Andrew Zisserman. Very deep convolutional networks for large-scale image recognition. In *IEEE conference on computer vision and pattern recognition*, 2014. 3
- [43] Marvin Teichmann, Michael Weber, Marius Zoellner, Roberto Cipolla, and Raquel Urtasun. Multinet: Real-time joint semantic reasoning for autonomous driving. In *IEEE Intelligent Vehicles Symposium*, 2018. 3
- [44] Paul Vernaza and Manmohan Chandraker. Learning random-walk label propagation for weakly-supervised semantic segmentation. In *IEEE conference on computer vision and pattern recognition*, 2017. 6
- [45] Lijun Wang, Huchuan Lu, Xiang Ruan, and Ming-Hsuan Yang. Deep networks for saliency detection via local estimation and global search. In *IEEE conference on computer vision and pattern recognition*, 2015. 2
- [46] Lijun Wang, Huchuan Lu, Yifan Wang, Mengyang Feng, Dong Wang, Baocai Yin, and Xiang Ruan. Learning to detect salient objects with image-level supervision. In *IEEE conference on computer vision and pattern recognition*, 2017. 5
- [47] Linzhao Wang, Lijun Wang, Huchuan Lu, Pingping Zhang, and Xiang Ruan. Saliency detection with recurrent fully convolutional networks. In *European conference on computer vision*, 2016. 2, 6
- [48] Xiang Wang, Shaodi You, Xi Li, and Huimin Ma. Weakly-supervised semantic segmentation by iteratively mining common object features. In *IEEE conference on computer vision and pattern recognition*, 2018. 1, 3, 6
- [49] Yunchao Wei, Jiashi Feng, Xiaodan Liang, Ming-Ming Cheng, Yao Zhao, and Shuicheng Yan. Object region mining with adversarial erasing: A simple classification to semantic segmentation approach. In *IEEE conference on computer vision and pattern recognition*, 2017. 1, 3, 5, 6
- [50] Yunchao Wei, Xiaodan Liang, Yunpeng Chen, Xiaohui Shen, Ming-Ming Cheng, Jiashi Feng, Yao Zhao, and Shuicheng Yan. Stc: A simple to complex framework for weakly-supervised semantic segmentation. *IEEE transactions on pattern analysis and machine intelligence*, 39(11):2314–2320, 2017. 1, 3, 6
- [51] Yunchao Wei, Huaxin Xiao, Honghui Shi, Zequn Jie, Jiashi Feng, and Thomas S Huang. Revisiting dilated convolution: A simple approach for weakly-and semi-supervised semantic segmentation. In *IEEE conference on computer vision and pattern recognition*, 2018. 1, 3, 6
- [52] Huaxin Xiao, Jiashi Feng, Yunchao Wei, and Maojun Zhang. Self-explanatory deep salient object detection. *arXiv preprint arXiv:1708.05595*, 2017. 1, 3
- [53] Dan Xu, Wanli Ouyang, Xiaogang Wang, and Nicu Sebe. Pad-net: Multi-tasks guided prediction-and-distillation network for simultaneous depth estimation and scene parsing. In *IEEE conference on computer vision and pattern recognition*, 2018. 3
- [54] Qiong Yan, Li Xu, Jianping Shi, and Jiaya Jia. Hierarchical saliency detection. In *IEEE conference on computer vision and pattern recognition*, 2013. 5
- [55] Chuan Yang, Lihe Zhang, Huchuan Lu, Xiang Ruan, and Ming-Hsuan Yang. Saliency detection via graph-based manifold ranking. In *IEEE conference on computer vision and pattern recognition*, 2013. 2

- [56] Yu Zeng, Mengyang Feng, Huchuan Lu, Gang Yang, and Ali Borji. An unsupervised game-theoretic approach to saliency detection. *IEEE Transactions on Image Processing*, 27(9):4545–4554, 2018. 1
- [57] Yu Zeng, Huchuan Lu, Lihe Zhang, Mengyang Feng, and Ali Borji. Learning to promote saliency detectors. In *IEEE Conference on Computer Vision and Pattern Recognition*, 2018. 1
- [58] Yu Zeng, Yunzhi Zhuge, Huchuan Lu, Lihe Zhang, Mingyang Qian, and Yizhou Yu. Multi-source weak supervision for saliency detection. In *IEEE Conference on Computer Vision and Pattern Recognition*, 2019. 1
- [59] Pingping Zhang, Dong Wang, Huchuan Lu, Hongyu Wang, and Xiang Ruan. Amulet: Aggregating multi-level convolutional features for salient object detection. In *IEEE international conference on computer vision*, 2017. 6
- [60] Pingping Zhang, Dong Wang, Huchuan Lu, Hongyu Wang, and Baocai Yin. Learning uncertain convolutional features for accurate saliency detection. In *IEEE international conference on computer vision*, 2017. 2, 6
- [61] Xiaoning Zhang, Tiantian Wang, Jinqing Qi, Huchuan Lu, and Gang Wang. Progressive attention guided recurrent network for salient object detection. In *IEEE conference on computer vision and pattern recognition*, 2018. 2, 6
- [62] Rui Zhao, Wanli Ouyang, Hongsheng Li, and Xiaogang Wang. Saliency detection by multi-context deep learning. In *IEEE conference on computer vision and pattern recognition*, 2015. 6
- [63] Bolei Zhou, Aditya Khosla, Agata Lapedriza, Aude Oliva, and Antonio Torralba. Learning deep features for discriminative localization. In *IEEE conference on computer vision and pattern recognition*, 2016. 1, 3
- [64] Yunzhi Zhuge, Yu Zeng, and Huchuan Lu. Deep embedding features for salient object detection. In *AAAI Conference on Artificial Intelligence*, 2019. 1